ORIGINAL PAPER

From elaborate to compact seasonal plant epidemic models and back: is competitive exclusion in the details?

**Ludovic Mailleret · Magda Castel ·
Josselin Montarry · Frédéric M. Hamelin**

Abstract Seasonality, or periodic host absence, is a central feature in plant epidemiology. In this respect, seasonal plant epidemic models take into account the way the parasite overwinters and generates new infections. These are termed primary infections. In the literature, one finds two classes of models: high-dimensional *elaborate* models and low-dimensional *compact* models, where primary infection dynamics are explicit and implicit, respectively. Investigating a compact model allowed previous authors to show the existence of a competitive exclusion principle. However, the way compact models derive from elaborate models has not been made explicit yet. This makes it unclear whether results such as competitive exclusion extend to elaborate models as well. Here, we show that assuming primary infection dynamics are fast in a standard elaborate model translates into a compact form. Yet, it is not that usually found in the literature. Moreover, we numerically show that coexistence is possible in this original compact form. Reversing the question, we show that the usual compact form approximates an alternate elaborate model, which differs from the earlier one in that primary infection dynamics are density dependent. We discuss to which extent these results shed light on coexistence within soil- and air-borne plant parasites, such as within the take-all disease of wheat and the grapevine powdery mildew cryptic species complexes, respectively.

Keywords Epidemiology · Semi-discrete model · Slow-fast dynamics · Model reduction · Chaos · Coexistence

L. Mailleret (✉)
UR 880 URIH INRA, 06903, Sophia Antipolis, France
e-mail: ludovic.mailleret@sophia.inra.fr

L. Mailleret
BIOCORE INRIA, 06902, Sophia Antipolis, France

M. Castel · J. Montarry · F. M. Hamelin
UMR 1099 BiO3P, INRA, Agrocampus Ouest
and Université de Rennes 1, 35042, Rennes, France

M. Castel
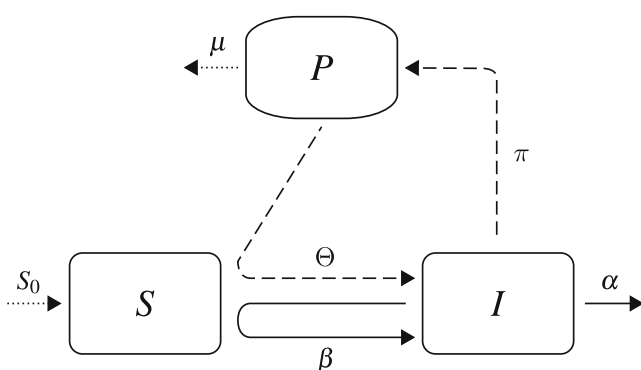e-mail: castel@agrocampus-ouest.fr

J. Montarry
e-mail: Josselin.Montarry@rennes.inra.fr

F. M. Hamelin
e-mail: fhamelin@agrocampus-ouest.fr

Introduction

Coexistence of closely related plant parasite species (or genetically distinct subgroups within a species) is ubiquitous (e.g., Fitt et al. 2006; Lebreton et al. 2007; Fournier and Giraud 2008; Montarry et al. 2008, 2009; Mougou et al. 2008; Mougou Hamdane et al. 2010; Daval et al. 2010). This apparently challenges the *competitive exclusion principle*, which states that "two species occupying the same ecological niche cannot coexist indefinitely" (Gause 1934; Chesson 2000). Ecological differences that lead to niche partitioning can occur in three basic ways: resource partitioning, temporal partitioning, and spatial partitioning (Wilson and Lindow 1994; Chesson 2000; Amarasekare 2003). Neither resource nor spatial partitioning seems to be involved in the coexistence of, e.g., the grapevine powdery mildew and the take-all disease of wheat cryptic

species complexes. Therefore, we wonder whether temporal niche partitioning would be a plausible explanation to coexistence in these species.

Under temperate climate, many plant parasites face seasonality, i.e., periodic absence of their host plant. This is brought about by winter environmental conditions which are unfavorable to the plants, so that, during this time period, many lose their vegetation (natural ecosystems) or are simply not cultivated (agricultural ecosystems). The periodical absence of the main primary producer species has consequences for the community supported by this producer. Compared to tropical zones, in which there is no such an abrupt seasonality, periodic host absence can induce major qualitative changes in plant parasite population dynamics, such as chaos (Shaw 1994). During the period of host absence, plant parasites overwinter through survival forms that can be particularly cold-resistant, e.g., cleistothecia for ascomycetes and oospores for oomycetes (Agrios 2005). These survival forms represent a source of *primary inoculum* since they will generate the first or *primary infections* the year after (see below as well). Only then can host-to-host or *secondary infections* occur. These secondary infections will in turn refill to some extent the primary inoculum reservoir, so as to face winter again (see Fig. 1; Table 1). Whether seasonality can promote temporal niche partitioning of plant parasite species remains an issue (Kiss et al. 2011).

There exists quite a diversity of plant epidemic models taking into account seasonal host absence and how parasites overwinter and generate primary and secondary infections (Gubbins and Gilligan 1997; Madden and van den Bosch 2007; Mailleret and Lemesle 2009,

Table 1 Notations

Label	Meaning
P	Primary inoculum density
S	Susceptible host plant density
I	Infected host plant density
τ	Growing season length (host plant is present)
$T - \tau$	Winter season length (host plant is absent)
T	Year length
β	Secondary infection rate
Θ	Primary infection rate
α	Infected host plants removal rate
π	Conversion rate from I to P (at the end of the season)
μ	Winter season mortality rate of primary inoculum
Λ	Primary inoculum density independent depletion rate
Ξ	Primary inoculum density dependent depletion rate

and references therein). A major distinguishing feature between these models concerns the way the primary inoculum pool is depleted. Once the parasite's overwintering form generates propagules that may come into contact with a susceptible host (e.g., spores, mycelium), it no longer belongs to the primary inoculum pool. However, depending on the biology of the parasite, such a depletion may occur as a response to host presence (Webb et al. 1999), or regardless as to whether susceptible hosts are actually present (Bailey and Gilligan 1999). For instance, many foliar parasites, such as the grapevine powdery mildew, have a primary inoculum form (cleistothecium) that releases *airborne* ascospores depending on the weather (rainfall and temperature), disregarding host presence, to possibly infect remote hosts (Gadoury and Pearson 1990; Gee et al. 2000). Another example is the potato late blight parasite: In *Phytophthora infestans*, oospore germination and the subsequent release of zoospores mostly depend on light and temperature (Harrisson 1992; Strömberg et al. 2001). Once released, the spores either come into contact with a host plant, or are lost. By contrast, many root parasites have a primary inoculum form that generates *soilborne* propagules upon reception of a chemical signal from the host. For instance, in the cyst nematodes, which overwinter in soil into the cyst form, populations hatch only when the host plant is present, through the action of root exudates (Fenwick 1949; Williams and Beane 1979; Rawsthorne and Brodie 1986). Another example is the oomycete *Aphanomyces euteiches*; Shang et al. (2000) showed indeed that root exudates of various plant species influence *A. euteiches* oospores germination. Accordingly, we will refer to the *soilborne* and *airborne* parasites models, to indicate that the primary inoculum depletion depends on the susceptible host density, or not, respectively.

Fig. 1 Schematic representation of the different epidemic processes in seasonal plant epidemic models with primary and secondary infection. *Dashed lines* figure primary infection-related processes, *plain lines* secondary infection ones, and *dotted lines* phenomena occurring between growing seasons. See Table 1 for notations

Such complex biological life cycles may lead to quite *elaborate* mathematical formulations (Truscott et al. 1997, 2000; Madden and van den Bosch 2002). Yet, more *compact* and mathematically tractable forms of seasonal plant epidemic models have recently been proposed (Madden and van den Bosch 2007; van den Berg et al. 2011). The essential difference between the elaborate and compact models lies in the explicit *versus* implicit nature of the primary infection modeling. Regarding coexistence of plant parasites in seasonal environments, van den Berg et al. (2011) showed that, in a class of compact models, a competitive exclusion principle holds. However, it is not clear whether this result holds for more elaborate models as well, e.g., Madden and van den Bosch (2002); it may still be that coexistence is possible in such models. To fill this gap in our understanding of plant parasite species coexistence, we will investigate and compare airborne and soilborne parasites ecological dynamics, through reducing each elaborate model to a mathematically more tractable compact form. Competitive exclusion and coexistence will then be numerically explored.

Airborne model

In this section, we consider airborne primary infection dynamics. That is, we assume that primary inoculum depletion early in the season occurs regardless as to whether host plants are actually present (see the "Introduction"). Hence, the per day primary inoculum loss rate Λ will be a constant.

We build on Madden and van den Bosch (2002)'s elaborate model, which explicitly considers both primary and secondary infection dynamics under environmental seasonality. This results in a three-dimensional *semi-discrete* model (Mailleret and Lemesle 2009); two sets of ordinary differential equations, coupled to two sets of recurrence equations, define the model. Assuming primary infections occur on a faster time scale than secondary infections, a slow–fast argument will show that the three-dimensional model is approximated by a two-dimensional semi-discrete model that is mathematically more tractable. We will further analyze the latter compact model.

Model equations

By "environmental seasonality," we refer to the succession of two time periods: the *growing season*, during which the host plant is present, and the *winter season*, say, during which the host plant is absent.

We let τ be the length of the growing season and T denote the year length. Thus, $(T - \tau)$ is the winter season length. Also, let (P, S, I) denote the primary inoculum, susceptible host plant, and infected host plant densities, respectively.

Let us start by considering the growing season. As usual, β and α denote the secondary infection and the infected host plants removal rates, respectively. Also, we let Θ denote the primary infection rate and Λ be the within-season primary inoculum loss rate. Thus, we let the k-th year's dynamics be governed by the following equation: For $t \in (kT, kT + \tau)$,

$$\dot{P} = -\Lambda P,$$
$$\dot{S} = -\Theta PS - \beta SI,$$
$$\dot{I} = +\Theta PS + \beta SI - \alpha I, \tag{1}$$

where the dot indicates derivative with respect to time t. The $\pm \Theta PS$ terms indicate that only a fraction of the released primary inoculum actually encounter healthy hosts and initiate primary infection, the remaining part being lost (Bailey and Gilligan 1999).

At the end of the growing season ($t = kT + \tau$), host plants are removed: e.g., crop plants are harvested, or leaves of deciduous trees fall down to the ground. At that time, infected host plants debris are assumed to convert into primary inoculum at a rate π (the parasite switches to a survival form). This translates into the following recurrence equation:

$$P(kT + \tau^+) = P(kT + \tau) + \pi I(kT + \tau),$$
$$S(kT + \tau^+) = 0,$$
$$I(kT + \tau^+) = 0, \tag{2}$$

where the $+$ superscript indicates the instant right after the end of the growing season.

During the winter season, host plants are absent and the parasites survive as primary inoculum (P), having a winter-specific mortality rate μ. Thus, for $t \in (kT + \tau, (k+1)T)$,

$$\dot{P} = -\mu P,$$
$$\dot{S} = 0,$$
$$\dot{I} = 0. \tag{3}$$

At the beginning of a new season ($t = (k+1)T$), new susceptible host plants are made available to the

parasite (crop plants are sowed or tree leaves emerge). Let their initial density be S_0. This translates into

$$P((k+1)T^+) = P((k+1)T),$$
$$S((k+1)T^+) = S_0,$$
$$I((k+1)T^+) = 0. \tag{4}$$

The semi-discrete model composed of sub-models 1 to 4 thus depicts the course of an epidemic over one cycle (1 year) through primary and secondary infection dynamics, infected host plants conversion into primary inoculum at the end of the season, and survival to host absence until the next year. This provides initial conditions for iterating a new cycle. It is Madden and van den Bosch (2002)'s model.

Fast primary infections

As suggested by Madden and van den Bosch (2002), let us assume primary infections occur on a faster time scale than secondary infections. This will allow us to approximate model 1–4 with a simpler form through slow–fast reduction techniques commonly used in ecology (Auger et al. 2008). Mathematically, this consists into letting $\lambda = \varepsilon\Lambda$ and $\theta = \varepsilon\Theta$, with $0 < \varepsilon \ll 1$; i.e., primary infection rate parameters Θ and Λ are assumed to take large values, compared to the secondary infection parameters β and α. Using this, one can rewrite Eq. 1 as

$$\varepsilon\dot{P} = -\lambda P,$$
$$\varepsilon\dot{S} = -\theta PS - \varepsilon\beta SI, \tag{5}$$
$$\varepsilon\dot{I} = +\theta PS + \varepsilon\beta SI - \varepsilon\alpha I,$$

with initial conditions at the beginning of year $(k+1)$:

$$P((k+1)T^+) = P((k+1)T),$$
$$S((k+1)T^+) = S_0, \tag{6}$$
$$I((k+1)T^+) = 0.$$

To take advantage of the assumption that primary infections are fast, i.e., that ε is small compared to 1, we now write Eq. 5 in an explicit slow–fast form. Let $t' = t/\varepsilon$ denote the fast time scale. After a little algebra, one gets

$$\frac{d}{dt'}\left(\log(S) - \frac{\theta}{\lambda}P\right) = -\varepsilon\beta I,$$
$$\frac{d}{dt'}(S+I) = -\varepsilon\alpha I,$$
$$\frac{d}{dt'}(P) = -\lambda P, \tag{7}$$

which is a slow–fast form of system 5 (Auger et al. 2008).

The theory of slow–fast dynamical systems tells us that, as long as ε is small, one can approximate the dynamics of system 5 by considering it on its slow manifold only, i.e., on the subset of the state space which attracts trajectories of the slow fast form of the system when ε is set to 0. This somehow corresponds to assuming that primary infections occur instantaneously.

For model 5, the slow manifold is determined by the attractor of Eq. 7, with $\varepsilon = 0$. It is thus characterized by the fact that $\left(\log(S) - \frac{\theta}{\lambda}P\right)$ and $(S+I)$ remain constant, while P goes exponentially to 0. Considering year $(k+1)$, the slow manifold of Eq. 5 is thus given by

$$P = 0,$$
$$\log(S) = \log(S_0) - \frac{\theta}{\lambda}P((k+1)T^+),$$
$$S + I = S_0. \tag{8}$$

Using the fact that (P, S, I) belongs to the slow invariant manifold (Eq. 8), we obtain the following model:

$$\dot{S} = -\beta SI,$$
$$\dot{I} = \beta SI - \alpha I, \tag{9}$$

with initial conditions

$$S((k+1)T^+) = S_0 \exp\left(-\frac{\theta}{\lambda}P((k+1)T^+)\right),$$
$$I((k+1)T^+) = S_0\left(1 - \exp\left(-\frac{\theta}{\lambda}P\left((k+1)T^+\right)\right)\right).$$
$$\tag{10}$$

(we omit $\dot{P}$ and P since both are equal to 0).

Model reduction

From Eqs. 2, 3, and 4, it is possible to further simplify Eqs. 9 and 10. It suffices to notice that Eqs. 3 and 4 translate into:

$$P((k+1)T^+) = e^{-\mu(T-\tau)}P(kT + \tau^+),$$

so that, using Eq. 2 and noticing that $P(kT + \tau) = 0$ (since the system is considered on the slow manifold (Eq. 8)), we have

$$P((k+1)T^+) = \pi e^{-\mu(T-\tau)}I(kT + \tau).$$

Using this last property in Eqs. 9 and 10, we end up with the following compact semi-discrete model: For all k and for any $t \in (kT, kT + \tau)$,

$$\dot{S} = -\beta SI,$$
$$\dot{I} = \beta SI - \alpha I, \tag{11}$$

coupled to the difference equation

$$S((k+1)T^+) = S_0 \exp\left(-\frac{\theta\pi e^{-\mu(T-\tau)}}{\lambda} I(kT+\tau)\right),$$

$$I((k+1)T^+) = S_0 \left(1 - \exp\left(-\frac{\theta\pi e^{-\mu(T-\tau)}}{\lambda} I(kT+\tau)\right)\right).$$

(12)

One easily sees that the compact model (Eqs. 11 and 12) is well-posed: that is, it cannot produce negative trajectories. Also, the latter remain bounded: S and I always remain smaller or equal to S_0. It is an original model (see "Linearized model" section to see how it relates to previous compact models).

In the limit that ε tends to 0, both the elaborate model (Eqs. 1–4) and the compact form (Eqs. 11 and 12) produce the same dynamics, while as ε remains small compared to 1, but not infinitely small, the compact form (Eqs. 11 and 12) provides a good approximation of the elaborate model (Eqs. 1–4) dynamics.

Notice that, due to the fast primary infections assumption and other features from the elaborate model, the compact semi-discrete model is independent of P
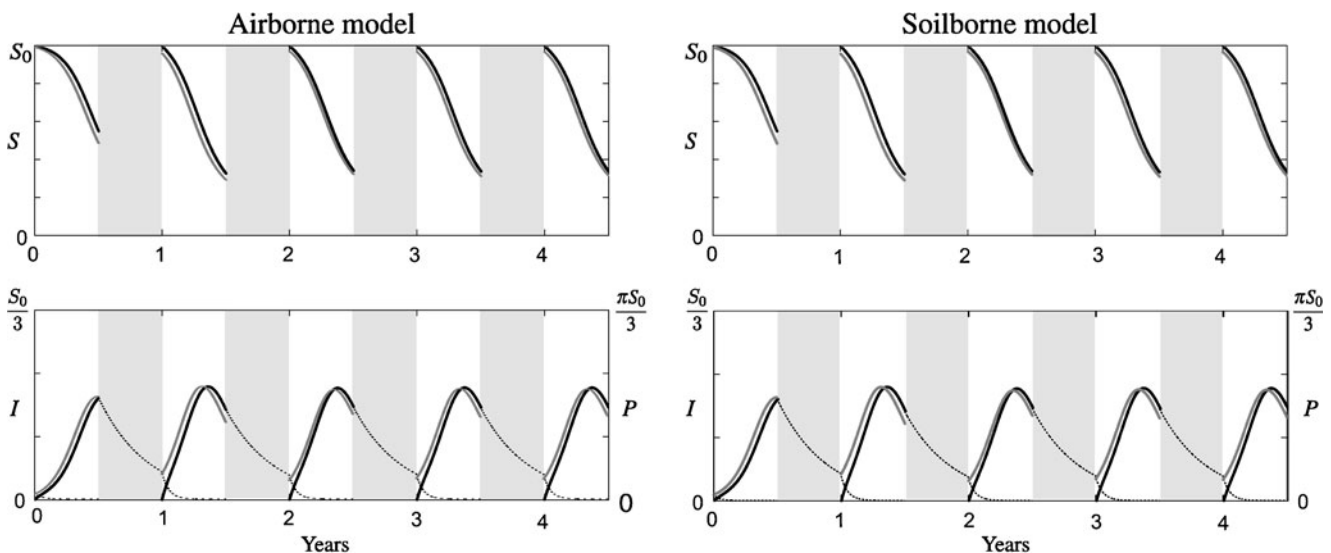
(the primary inoculum). This reduces the dimension of the model yet induces a time-gap during the winter season regarding the visual output (for $t \in (kT+\tau, (k+1)T)$, the compact model shows no solution; Fig. 2.)

Linearized model

Assuming $\theta\pi e^{-\mu(T-\tau)}/\lambda$ is small, Eq. 12 reads:

$$S((k+1)T^+) \cong S_0 - \frac{\theta\pi e^{-\mu(T-\tau)}}{\lambda/S_0} I(kT+\tau),$$

$$I((k+1)T^+) \cong \frac{\theta\pi e^{-\mu(T-\tau)}}{\lambda/S_0} I(kT+\tau).$$

(13)

The linearity in the discrete part makes model 11–13 essentially equivalent to Madden and van den Bosch (2007) and van den Berg et al. (2011). This shows a limit to van den Berg et al. (2011)'s result concerning the existence of a competitive exclusion principle in airborne parasites which is strongly dependent on the linearity of the discrete part. It is actually unclear how small $\theta\pi e^{-\mu(T-\tau)}/\lambda$ has to be (i.e., how inefficient primary

Fig. 2 Two epidemic dynamics for the take-all disease of wheat over 5 years, from airborne (*left*) and soilborne (*right*) models. Compact model (Eqs. 11 and 12) simulations are represented in *gray lines*, and full model (Eqs. 1–4) simulations are represented in *black solid lines*. In the *bottom row*, *solid lines* represent infected host plant density I, while the *dotted lines* represent primary inoculum density P. Winter seasons are illustrated with *light-shaded areas*. Parameters were $\tau = 184$ days, $T = 365$ days (van den Berg et al. 2011), $S_0 = 1$ arbitrary host plant unit, $\beta = 0.04875$ per day per host plant (root fragment) unit (van den Berg et al. 2011)'s $\beta K/2$, taking host density at the inflexion point)

$\alpha = 0.024$ per day (van den Berg et al. 2011), $\pi = 1$ arbitrary primary inoculum unit per host plant unit (each infectious root fragment is a potential primary inoculum unit), $\mu = 0.0072$ per day (van den Berg et al. 2011), $\Lambda = 0.052$ per day (Bailey and Gilligan (1999)'s r_d), $\Theta = 0.04875$ per primary inoculum unit per day (similar to β, primary inoculum units being also root fragments) and $\xi = \lambda/S_0$ per day per host unit. Initial conditions were $S(0) = S_0$, $I(0) = 0$, $P(0) = 0.01$ (elaborate model), or computed from Eq. 10 with $P((k+1)T^+) = P(0)$ from the elaborate model (compact model)

inoculum has to be), for the approximation 13 to remain valid and thus for the competitive exclusion principle to hold.

$\mathscr{R}_0$ derivation

We define the parasite's *basic reproduction number* $\mathscr{R}_0$ as the quantity of primary inoculum at the beginning of year $(k + 1)$ produced via the infections generated by one primary inoculum unit at the beginning of year k, in a disease-free context (Diekmann and Hesterbeek 2000; Madden and van den Bosch 2002, 2007; van den Bosch et al. 2008). Mathematically speaking, $\mathscr{R}_0$ will thus be computed as $P((k + 1)T^+)/P(kT^+)$ estimated from the linearized dynamics around the disease-free solution. Since winters are implicit in the compact form (Eqs. 11 and 12), the disease-free solution is actually an equilibrium and not a stationary cycle, yet it should be kept in mind that plant populations do cycle (they are absent during winters) even though it is not apparent in the aggregated model equations.

We now state the following result regarding the stability of the disease-free equilibrium in the compact model. The proof is in "Appendix 1".

Theorem 1 *The compact model* (Eqs. 11 and 12) *admits a stationary disease-free solution* $(S, I) = (S_0, 0)$ *which is globally asymptotically stable (GAS) if and only if the parasite's basic reproduction number*

$$\mathscr{R}_0 = \frac{\theta \pi e^{-\mu(T-\tau)}}{\lambda} e^{(\beta S_0 - \alpha)\tau} S_0,$$

is smaller or equal to 1.

Numerical computations

To investigate the dynamical behavior of the airborne model, we performed some numerical simulations of the elaborate and compact forms when $\mathscr{R}_0 > 1$. We most of the time identified a, seemingly GAS, periodic stationary solution of period 1 year, i.e., characterized by the exact replication of the epidemic from one season to the other. Figure 2's left panel shows such dynamics in which, after a transient, the epidemic reaches a periodic behavior.

Elaborate and compact models comparison

To illustrate the model reduction's relevance, Fig. 2's left panel shows both the compact and elaborate model dynamics. The parameter set was chosen to fit the take-
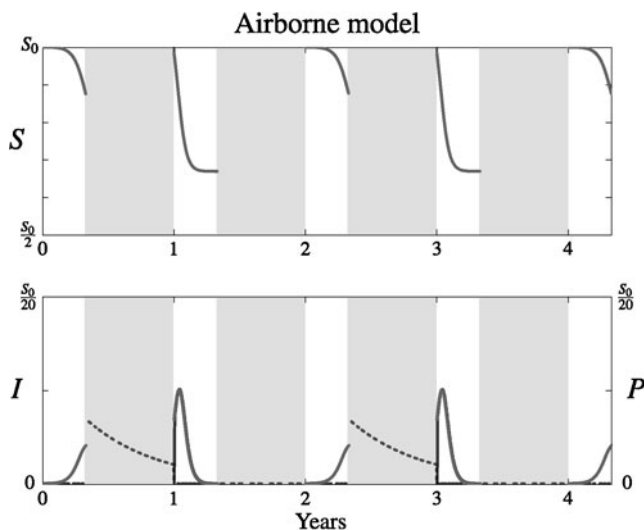
all disease of wheat (caused by the soilborne fungus *Gaeumannomyces graminis* var. *tritici*), for which realistic parameter values exist in the literature (Bailey and Gilligan 1999; van den Berg et al. 2011). This will allow us to compare airborne and soilborne mathematical models, given a parameter set.

Regarding the airborne model, even though Θ and Λ are not that small compared to β and α (i.e., primary infections are not that fast), the compact model provides a good approximation of the elaborate model dynamics.
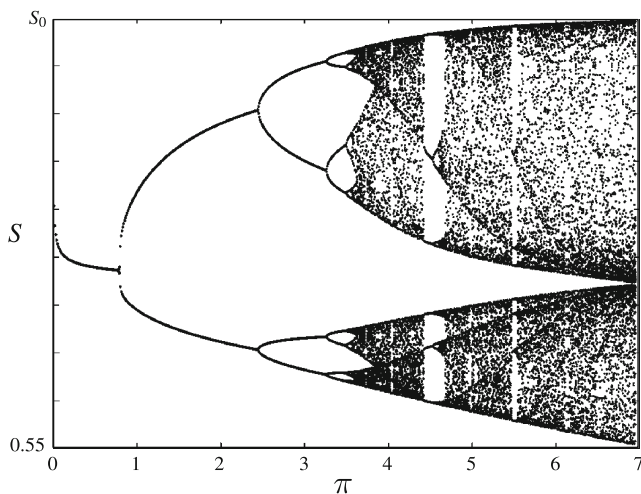
The route to chaos

It is well-known that complicated dynamics (such as chaos) may easily arise in semi-discrete models and that seasonal plant epidemic models may produce such patterns as well (Mailleret and Lemesle 2009; Shaw 1994). We thus performed bifurcation analyzes to investigate whether or not the airborne model can exhibit such dynamics. We were actually not able to find any bifurcation starting from the parameters used in the simulations presented on Fig. 2. Yet, with other parameter values, 2-year periodic epidemic dynamics were observed (Fig. 3). Such dynamics results from the succession from 1 year to the next of under- and over-exploitation phases of healthy hosts by the parasite. Indeed, at the beginning of the first year of a $2T$ period cycle (Fig. 3), there are very few parasites; they exploit the healthy hosts very efficiently through primary and secondary infection, yielding an important amount of primary inoculum at the end of the growing season. This high primary inoculum density results in a quite large number of infected hosts after the second year's primary infection phase. Then, the number of healthy hosts rapidly fall below the threshold $\frac{\alpha}{\beta}$, and new-infected hosts cannot compensate for disease-induced host mortality. Consequently, very few infected hosts survive until the end of the season, which results in a very small parasite density at the beginning of the next season, and the cycle is over.

To go deeper into the analysis, we focused on the compact model. Keeping the same parameters as in Fig. 3, we varied π from 0 to 7 primary inoculum unit per host plant unit. This unveiled a transition from periodic solutions of period 1 year to chaotic regimes through a cascade of period doubling bifurcations (see Fig. 4), which is a very classical route to chaos (Guckenheimer and Holmes 2002). We must note, however, that the parameter values at which the bifurcations appeared correspond to quite large $\mathscr{R}_0$ values: on Fig. 4, $\mathscr{R}_0$ ranges from 0 ($\pi = 0$) to almost 10^3 ($\pi = 7$). This implies that such complicated dynamical

Airborne model

Fig. 3 Example of a 2-year period stationary solution of the airborne model. Graphic code is similar to the one described in Fig. 2. Parameters were $\tau = 120$ days, $T = 365$ days, $S_0 = 1$ arbitrary host plant unit, $\beta = 0.43$ per day per host plant unit, $\alpha = 0.3698$ per day, $\mu = 0.005$ per day, $\lambda = 0.2938$ per day, $\theta = 0.1$ per primary inoculum unit per day $\pi = 1.7$, and $\varepsilon = .1$, for the elaborate model simulation

Fig. 4 Bifurcation diagram for the compact form of the airborne model (Eqs. 11 and 12). Each *dot* of the figure represents an asymptotic of S at the end of the growing season, computed from the 50 last years of a 600-year simulation (to remove the transients), against parameter π. Parameters were as in Fig. 3 except that π was varied from 0 to 7 primary inoculum unit per host plant unit. The bifurcation associated with the emergence of a positive globally stable T-periodic solution ($\mathscr{R}_0$ just above 1) happens for very low values of π (≈ 0.007) so that it is not visible on the picture. The transition from this globally stable periodic solution to chaos occurs through a cascade of period doubling bifurcations
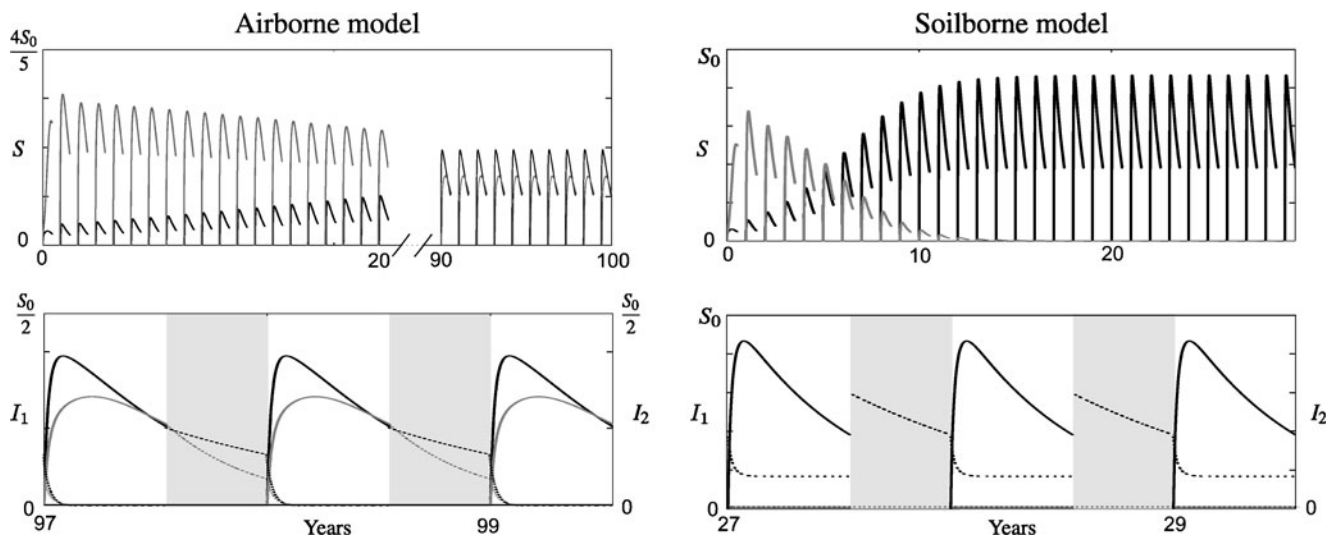
patterns may be difficult to encounter in nature, since such high reproductive abilities are arguably hardly met by any plant parasite.

Since it may have happened that the bifurcations we observed were artifacts induced by the slow–fast model reduction, we computed the same bifurcation diagram for the elaborate airborne model with $\varepsilon = 0.1$. We actually observed a pattern mostly similar to the one shown on Fig. 4, except that the different bifurcations occurred for slightly larger values of π. This is because the reduction of the primary infection phase tends to make the pathogen a little more efficient during primary infection (see S dynamics on Fig. 2's left panel, where the compact approximation always slightly underestimates healthy hosts density in the elaborate model). Thus, the compact model is more prone to over-exploitation phenomena, which are responsible for period doubling bifurcations.

Coexistence issue

To show that two strains can coexist, we assumed one strain performs better than the other within the growing season and the other way around during the winter season; this is supported by empirical evidence in several ecological models (Carson 1998; Abang et al. 2006). Mathematically, this translated into considering two sets of variables I_i, P_i ($i = 1, 2$), representing the two parasite strains, with dynamics following the same functional form as in model 1–4. All parameters were assumed equal for the two strains except μ_i and β_i to reflect their different between and within season performances. The only other change is that $\dot{S} = -\sum_i (\Theta SP_i - \beta_i SI_i)$ in Eq. 1 to take into account that susceptible hosts may be infected by strain 1 or by strain 2. Figure 5's left panel numerically shows that coexistence of two strains is theoretically possible in the airborne model. Although simulations were realized for an ad hoc parameter set, the fact that the basic reproduction number takes different values for strain 1 and for strain 2 suggests this is not a degenerate case.
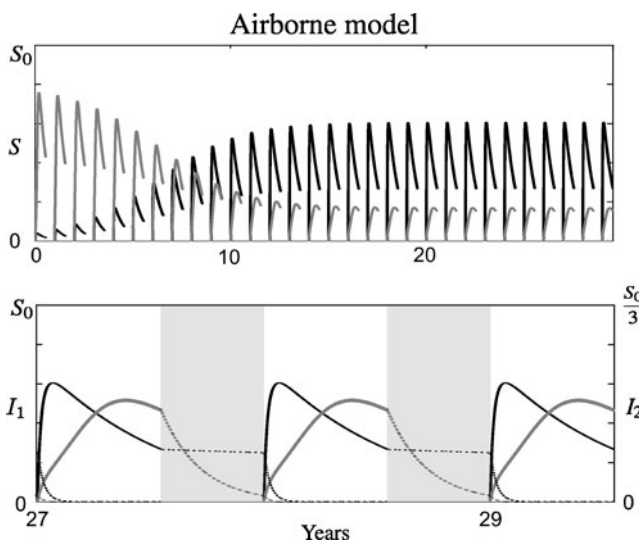
Moreover, Fig. 6 shows another instance of coexistence; the epidemic dynamics are typical of those observed regarding the grapevine powdery mildew, *Erysiphe necator*, for which two genetically distinct parasite strains coexist. Montarry et al. (2008, 2009) showed that niche partitioning, allowing the coexistence of two genetically differentiated groups of *E. necator* isolates (A and B) on the same host (i.e., the same resource, *Vitis vinifera*), results from a separation in time (and not in space). The groups temporal dynamics showed that group A isolates were active only at

Fig. 5 Two epidemic dynamics of two parasite strains in competition (I_1 and I_2) simulated from both the elaborate airborne model (*left column*) and the elaborate soilborne model (*right column*). The *bottom row* zooms on the last 3 years. Infected plant densities I_1 and I_2 are represented by *black* and *gray solid lines*, respectively. In the *bottom row*, the *dotted lines* represent primary inoculum densities P_1 and P_2; winter seasons are illustrated with *light-shaded areas*. Parameters were $T = 200$ days,

$\tau = 165$ days, $S_0 = 1$ arbitrary host plant unit, $\alpha = 0.005$ per day, $\pi = 1$ arbitrary primary inoculum unit per host plant unit, $\theta = 0.5$, $\lambda = 0.1$ per day (*left*), and $\xi = \lambda/S_0$ per day per host unit (*right*); I_1 and I_2 were parameterized by $\beta_1 = 0.01 < \beta_2 = 0.035$ and $\mu_1 = 0.0025 < \mu_2 = 0.0068$, respectively. Initial conditions were $S(0) = S_0$, $I_1(0) = 0$, $I_2(0) = 0$, $P_1(0) = 0.01$, and $P_2(0) = 0.01$

the beginning of the growing season and disappeared during the course of the epidemic, whereas group B isolates were responsible for late infections.

Fig. 6 Epidemic dynamics of two parasite strains in competition (I_1 and I_2) simulated from both the elaborate airborne model. The *bottom row* zooms on the last 3 years. Infected plant densities I_1 and I_2 are represented by *black* and *grey solid lines*, resp. In the *bottom row*, the *dotted lines* represent primary inoculum densities P_1 and P_2; winter seasons are illustrated with *light-shaded areas*. Parameters were as in Fig. 5, except for $\lambda = 0.1$ per day, $\beta_1 = 0.001 < \beta_2 = 0.1$ per day per host plant unit, and $\mu_1 = 0.0004 < \mu_2 = 0.0158$ per day

Soilborne model

In this section, we consider soilborne primary infection dynamics. That is, we consider that primary inoculum depletion occurs *only* in the presence of (or contact with) susceptible host plants (see the "Introduction").

Let Ξ denote a healthy host density-dependent primary inoculum depletion rate. Taking into account this feature rather than density-independent depletion, Eq. 1 reads:

$$\dot{P} = -\Xi PS,$$
$$\dot{S} = -\Theta PS - \beta SI,$$
$$\dot{I} = +\Theta PS + \beta SI - \alpha I. \qquad (14)$$

Equations 2–4 remain unchanged. The above equation is Webb et al. (1999)'s model, although these authors did not include it in a seasonal framework.

Model reduction

The soilborne model reduction under the assumption that primary infections are fast, i.e., that Ξ and Θ are large compared to the other parameters, is reported in "Appendix 2."

Proceeding as for the airborne model, we obtain the following compact semi-discrete model, which approx-

imates the soilborne model composed of Eqs. 14, 2, 3, and 4: for all k and for any $t \in (kT, kT + \tau)$,

$$\dot{P} = 0,$$
$$\dot{S} = -\beta SI,$$
$$\dot{I} = \beta SI - \alpha I, \qquad (15)$$

coupled to the difference equations

$$P((k+1)T^+) = \max\left(0, \pi e^{-\mu(T-\tau)}I(kT+\tau) - \frac{\xi}{\theta}S_0\right),$$

$$S((k+1)T^+) = \max\left(S_0 - \frac{\theta}{\xi}\pi e^{-\mu(T-\tau)}I(kT+\tau), 0\right),$$

$$I((k+1)T^+) = \min\left(\frac{\theta}{\xi}\pi e^{-\mu(T-\tau)}I(kT+\tau), S_0\right). \quad (16)$$

Again, the compact form of the soilborne models 15 and 16 is well-posed: S, I, and $(S + I)$ are constrained to the set $[0, S_0]$. "When linearity stems from model reduction" section shows how it relates to previous models.

Notice that, in this model, all healthy host plants may be infected during the fast primary infection phase. Also, primary inoculum is not necessarily entirely depleted after the fast primary infection phase. In biological words, there may be enough primary inoculum at the beginning of year $(k + 1)$ to infect all healthy host through primary infections (this can also be interpreted in terms of high primary inoculum infection ability ξ, or in terms of low healthy host density S_0). Such a situation is linked to the density-dependent primary inoculum decay rate: as P infect healthy hosts S, the rate at which P are depleted also decreases, which makes it possible to infect more healthy hosts than in the airborne model. Primary inoculum is thus more efficient in the soilborne model, due to density dependence.

When linearity stems from model reduction

In the situation where all the primary inoculum is systematically depleted after the primary infection phase, i.e., as long as primary inoculum cannot infect all healthy host plants through primary infections (which seems a biologically reasonable case), one gets, for $t \in (kT, kT + \tau)$, the following form where the discrete part is linear

$$\dot{S} = -\beta SI,$$
$$\dot{I} = \beta SI - \alpha I, \qquad (17)$$

coupled to the difference equations

$$S((k+1)T^+) = S_0 - \frac{\theta}{\xi}\pi e^{-\mu(T-\tau)}I(kT+\tau),$$

$$I((k+1)T^+) = \frac{\theta}{\xi}\pi e^{-\mu(T-\tau)}I(kT+\tau). \qquad (18)$$

This simplification of the discrete part of the model may occur in many different cases, for instance when $\mathcal{R}_0 \leq 1$ (see "Appendix 2"), when either S_0, μ, or ξ is large or when either π or θ is small.

Interestingly, the linearity in the discrete part makes models 17 and 18 essentially equivalent to Madden and van den Bosch (2007) and van den Berg et al. (2011). Thus, our analysis provides a "mechanistic underpinning" of these models (Geritz and Kisdi 2004), based on the explicit consideration of both seasonality (periodic host absence) and primary infection dynamics.

$\mathcal{R}_0$ derivation

As in the airborne model, we get the following result linking the parasite's basic reproduction number $\mathcal{R}_0$ and the stability of the disease-free equilibrium. The proof is presented in "Appendix 3."

Theorem 2 *The compact model* (Eqs. 15 and 16) *admits a stationary disease-free solution* $(S, I) = (S_0, 0)$ *which is GAS if and only if the parasite's basic reproduction number*

$$\mathcal{R}_0 = \frac{\theta\pi e^{-\mu(T-\tau)}}{\xi}e^{(\beta S_0 - \alpha)\tau}.$$

is smaller or equal to 1.

Numerical computations

Comparing the airborne and soilborne models

Proceeding as in "Airborne model" section, we performed some numerical simulations of the soilborne model. To begin with, we show on Fig. 2's right panel epidemic dynamics converging toward a periodic stationary solution of period 1 year. To make things comparable, we set all the parameters common to the airborne and soilborne models to the same values than in Fig. 2's left panel. Moreover, we set ξ to the same numerical value than λ; since $S_0 = 1$, this implies that $\mathcal{R}_0$ are the same on the left and right panel of Fig. 2. The dynamics produced by the soilborne model are almost identical to those of the airborne model. This is due to the fact that, for this parameter set, S does not vary that much during the primary infection phase (i.e.,

$\xi S \approx \xi S_0 = \lambda$), making density dependence apparently transparent.

Regarding chaos

We also proceeded to a bifurcation analysis for the compact form of the soilborne model, once again choosing the same parameter values than for the airborne model and letting ξ being equal to the numerical value of λ for the airborne model (Fig. 4), which resulted in comparing models with the same $\mathscr{R}_0$. We obtained a bifurcation diagram very similar to the airborne model's one (Fig. 4), except that the bifurcation occurred for slightly lower values of the parameter π. This is caused by primary inoculum being more efficient in the soilborne model, which renders the system more prone to over-exploitation phenomena and thus to bifurcations ("The route to chaos" section). Again, as for the airborne model, we observed the same bifurcation diagram for the elaborate form of the soilborne model with $\varepsilon = 0.1$, except that bifurcations occurred for slightly larger values of the parameter π.

Coexistence issue

To investigate the two-strain dynamics, we proceeded as for the airborne model, regarding the two-strain model. Figure 5's right panel numerically illustrates the competitive exclusion principle van den Berg et al. (2011) found regarding the compact form of the model, by showing that it holds in the associated soilborne elaborate model. However, one sees that this does not hold anymore in the airborne model (Fig. 5's left panel), everything else being unchanged. Therefore, although Fig. 2 indicates that there is little quantitative difference in the take-all disease dynamics between airborne and soilborne models, the structural differences arise when looking at the qualitative dynamics in a broader ecological context. In other words, our study shows that density dependence in the primary inoculum depletion rate, which is typical of soilborne diseases, may prevent species coexistence.

Discussion

Two three-dimensional semi-discrete models, named "airborne" and "soilborne" models, were investigated. Both models combine seasonality (periodic host absence) and explicit primary infection dynamics, as in Madden and van den Bosch (2002). Airborne and soilborne models differ in that the primary inoculum depletion rate is density independent and depen-

dent, respectively (Webb et al. 1999). Assuming primary infections are fast, reduction techniques (Auger et al. 2008) allowed us to derive two two-dimensional model approximations that are mathematically more tractable.

A first issue was whether one recovers a simple semi-discrete model whose continuous part is the standard SIR model (Smith 2008) and whose discrete part is linear, as in Madden and van den Bosch (2007) and van den Berg et al. (2011). One ecological implication comes from the fact that the latter authors showed a competitive exclusion principle holds in such a model. That is, the parasite strain having the largest epidemiological basic reproduction number R_0, defined in "Appendix 4", eventually wins the competition; the other strains die out. Long run coexistence is thus impossible in such a model.

In both airborne and soilborne models, applying the aforementioned reduction technique led to a continuous SIR part, yet to a generally nonlinear discrete part. Regarding the airborne model, "Linearized model" section showed that it can be linearized in the limit of an infinitely small composite parameter. As for the soilborne model, "When linearity stems from model reduction" section showed that it simplifies to a linear discrete part very similar to Madden and van den Bosch (2007) and van den Berg et al. (2011) in a significant part of the parameter space.

On the one hand, this indicates that long-run persistence is unlikely in the soilborne model. Yet, there is no lack of empirical counterexamples, e.g., for the take-all disease of wheat (Lebreton et al. 2007; Daval et al. 2010). A simple explanation to that apparent paradox is that *G. graminis* var. *tritici*, although being a soilborne plant parasite, better fits the airborne model because it releases propagules (free-living mycelium, which grows in the soil) regardless of host (wheat roots) presence (Bailey and Gilligan 1999). This allows us to stress that the so named airborne and soilborne models do not necessarily correspond to the biologically very diverse airborne and soilborne plant parasites, respectively.

On the other hand, we numerically showed that long run coexistence is possible in the airborne model. This is supported by experimental evidence, such as within the powdery mildew species complex ("Coexistence issue" section). The theoretical investigation of the evolution of plant parasites in seasonal environments is currently receiving increased attention (van den Berg et al. 2010, 2011). Yet these studies are based on epidemic models in which a competitive exclusion principle holds, what tremendously restricts the possible outcomes of natural selection. Future research should thus address the evolutionary implications of systems

allowing more complex behaviors, such as co-existence of different parasite species, like, e.g., in the present airborne model.

Appendix 1: Proof of theorem 1

It is easy to see that $(S, I) = (S_0, 0)$ is a stationary solution of Eq. 11, so that $I(kT + \tau) = 0$, which used in Eq. 12, implies that at the beginning of year $(k + 1)$, $S((k + 1)T^+) = S_0$ and $I((k + 1)T^+) = 0$. Therefore, the disease-free solution $(S, I) = (S_0, 0)$ is an equilibrium of models 11 and 12.

Linearizing Eqs. 11 and 12 around $(S, I) = (S_0, 0)$, yields

$$I(kT + \tau) = e^{(\beta S_0 - \alpha)\tau} I(kT^+),$$
$$= e^{(\beta S_0 - \alpha)\tau} S_0 \frac{\theta \pi e^{-\mu(T-\tau)}}{\lambda} I((k-1)T + \tau),$$

so that, remembering that $P((k+1)T^+) = \pi e^{-\mu(T-\tau)} I(kT + \tau)$ and rearranging the terms, we get

$$\mathcal{R}_0 = \frac{P((k+1)T^+)}{P(kT^+)} = \frac{\theta \pi e^{-\mu(T-\tau)}}{\lambda} e^{(\beta S_0 - \alpha)\tau} S_0.$$

Consider Eq. 11. Since S is always upper-bounded by S_0, we have, for $t \in (kT, kT + \tau)$,

$$\dot{I} \le (\beta S_0 - \alpha) I \implies I(kT + \tau) \le e^{(\beta S_0 - \alpha)\tau} I(kT^+),$$

so that, using Eq. 12, we have:

$$I((k+1)T^+)$$
$$\le S_0 \left(1 - \exp\left(-\frac{\theta \pi e^{-\mu(T-\tau)}}{\lambda} e^{(\beta S_0 - \alpha)\tau} I(kT^+) \right) \right).$$

The right-hand side of the previous equation is an increasing, strictly concave, function of $I(kT^+)$ which equals 0 for $I(kT^+) = 0$ with a slope equal to

$$S_0 \frac{\theta \pi e^{-\mu(T-\tau)}}{\lambda} e^{(\beta S_0 - \alpha)\tau} = \mathcal{R}_0$$

around $I(kT^+) = 0$. Classical results on one-dimensional recurrence equations allows one to conclude that if $\mathcal{R}_0$ is smaller or equal to 1, the sequence $(I(kT^+))_{k \in \mathbb{N}}$ is decreasing and converges to 0 as k goes to infinity.

A similar argument can be used for the sequence $(S_0 - S(kT^+))_{k \in \mathbb{N}}$, showing that, if $\mathcal{R}_0 \le 1$, the sequence $(S(kT^+))_{k \in \mathbb{N}}$ is increasing and converges to S_0 as k goes to infinity. Thus, the disease-free solution $(S_0, 0)$ is globally attractive provided $\mathcal{R}_0 \le 1$. On one hand, the monotonicity of both sequences $(I(kT^+))_{k \in \mathbb{N}}$ and $(S(kT^+))_{k \in \mathbb{N}}$ also implies that $(S_0, 0)$ is locally stable if $\mathcal{R}_0 \le 1$. On the other hand, the consideration of models 11 and 12 linearized around $(S_0, 0)$ easily allows one to conclude that the disease-free solution is unstable if $\mathcal{R}_0 > 1$. This concludes the proof that $(S_0, 0)$ is GAS if and only if $\mathcal{R}_0 \le 1$.

Appendix 2: Fast primary infections in the soilborne model

Proceeding as for the airborne model, let $\xi = \varepsilon \Xi$. Equation 14 reads, in an explicit slow–fast form:

$$\frac{d}{dt'}\left(S - \frac{\theta}{\xi} P \right) = -\varepsilon \beta S I,$$

$$\frac{d}{dt'}(S + I) = -\varepsilon \alpha I,$$

$$\frac{d}{dt'}(P) = -\xi P \left(\left(S - \frac{\theta}{\xi} P \right) + \frac{\theta}{\xi} P \right). \quad (19)$$

Thus, the slow manifold of system 19 is characterized by the fact that $\left(S - \frac{\theta}{\xi} P \right)$ and $(S + I)$ remain constant.

During year $(k + 1)$, according to Eq. 4, these constants are equal to $\left(S_0 - \frac{\theta}{\xi} P((k+1)T^+) \right)$ and S_0, respectively. Taking this into account and letting ε tend to 0, we get that the fast dynamics of P are determined by:

$$\frac{d}{dt'}(P) = -P \left((\xi S_0 - \theta P((k+1)T^+)) + \theta P \right), \quad (20)$$

which is a quadratic differential equation with two equilibria

$$P_1 = 0, \text{ and } P_2 = P((k+1)T^+) - \frac{\xi}{\theta} S_0,$$

the latter being positive or negative depending on S_0, ξ, θ, and $P((k+1)T^+)$. Actually, the sign of P_2 also determines which equilibrium is an attractor.

If $P_2 \leq 0$, $P_1 = 0$ is an attractor of the fast Eq. 20 for positive initial conditions, the slow manifold reduces to the set

$$P = 0,$$
$$S = S_0 - \frac{\theta}{\xi} P((k+1)T^+),$$
$$I = \frac{\theta}{\xi} P((k+1)T^+).$$

If $P_2 > 0$, then $P_2 = \left(P((k+1)T^+) - \frac{\xi}{\theta} S_0\right)$ is an attractor of the fast Eq. 20 for positive initial conditions. In that case, the slow manifold of Eq. 19 is the set

$$P = \left(P((k+1)T^+) - \frac{\xi}{\theta} S_0\right),$$
$$S = 0,$$
$$I = S_0.$$

It is actually possible to summarize these two cases using the max and min functions. One obtains that the slow manifold of system 19 is the set

$$P = \max\left(0, P((k+1)T^+) - \frac{\xi}{\theta} S_0\right),$$
$$S = \max\left(S_0 - \frac{\theta}{\xi} P((k+1)T^+), 0\right),$$
$$I = \min\left(\frac{\theta}{\xi} P((k+1)T^+), S_0\right). \quad (21)$$

In these notations, either P, S, and I are all equal to the first argument of the functions max or min, respectively, or are all equal to the second.

Appendix 3: Proof of theorem 2

We compute the basic reproduction number in models 15 and 16 from the linearization of the model around the disease-free equilibrium $(S_0, 0)$; we easily obtain

$$\mathcal{R}_0 = \frac{P((k+1)T^+)}{P(kT^+)} = \frac{\theta \pi e^{-\mu(T-\tau)}}{\xi} e^{(\beta S_0 - \alpha)\tau}.$$

As in the airborne model, it is fairly easy to show that $(S_0, 0)$ is a stationary solution of models 15 and 16.

Consider $\dot{I}$ in Eq. 15. Remembering that $(S + I)$ is restricted to $[0, S_0]$, we have $\forall t \in (kT, kT + \tau)$,

$$\dot{I} \leq \beta(S_0 - I)I - \alpha I = (\beta S_0 - \alpha)\left(1 - \frac{\beta I}{\beta S_0 - \alpha}\right) I,$$

Exploiting order preserving flow properties of one-dimensional ordinary differential equations and separation of variables techniques, we get

$$I(kT + \tau) \leq \frac{(\beta S_0 - \alpha)e^{(\beta S_0 - \alpha)\tau} I(kT^+)}{(\beta S_0 - \alpha) + \beta(e^{(\beta S_0 - \alpha)\tau} - 1)I(kT^+)}. \quad (22)$$

We shall now use the third equation in Eq. 16 to compute $I((k+1)T^+)$, but the nonlinear min function requires some attention. One can easily show that $I(kT + \tau) \leq e^{(\beta S_0 - \alpha)\tau} S_0$. Thus

$$\frac{\theta}{\xi} \pi e^{-\mu(T-\tau)} I(kT+\tau) \leq \frac{\theta}{\xi} \pi e^{-\mu(T-\tau)} e^{(\beta S_0 - \alpha)\tau} S_0 = \mathcal{R}_0 S_0,$$

so that if $\mathcal{R}_0 \leq 1$, we have

$$\min\left(\frac{\theta}{\xi} \pi e^{-\mu(T-\tau)} I(kT+\tau), S_0\right) = \frac{\theta}{\xi} \pi e^{-\mu(T-\tau)} I(kT+\tau).$$

Assume from now on $\mathcal{R}_0 \leq 1$. Using Eq. 22 and the previous remark, we get

$$I((k+1)T^+) \leq \frac{\frac{\theta}{\xi} \pi e^{-\mu(T-\tau)} (\beta S_0 - \alpha)e^{(\beta S_0 - \alpha)\tau} I(kT^+)}{(\beta S_0 - \alpha) + \beta(e^{(\beta S_0 - \alpha)\tau} - 1)I(kT^+)}.$$

As in "Appendix 1" the right-hand side of the previous equation is an increasing, strictly concave, function of $I(kT^+)$ which equals 0 for $I(kT^+) = 0$ with a slope equal to

$$\frac{\theta \pi e^{-\mu(T-\tau)}}{\xi} e^{(\beta S_0 - \alpha)\tau} = \mathcal{R}_0$$

at $I(kT^+) = 0$. Concluding that $(S_0, 0)$ is globally attractive for trajectories of models 15 and 16 if $\mathcal{R}_0 \leq 1$ is no harder than in the airborne case, nor is the local (un)stability study.

Appendix 4: Alternate $\mathcal{R}_0$ definition and evolutionary implications

Using a technique introduced by Bacaer and Guernaoui (2006) to study periodic epidemic models, the parasite's basic reproductive number can be derived alternately. Let us focus on the airborne model. A similar derivation can be made regarding the soilborne model, *mutatis mutandis*. Let us linearize Eqs. 11 and 12 around the disease-free equilibrium $(S_0, 0)$ at first order in s and i, with $(S, I) = (S_0 + s, i)$. Since for all $t \in (kT + \tau, (k+1)T)$ models 11 and 12 define no solution (the time-gap mentioned in the body of the paper), we find convenient to make the following

time change: Let $z = t - (k - 1)(T - \tau)$, with $k \in \mathbb{N}^*$. We get, for the continuous part: $\forall z \in [k\tau, (k+1)\tau)$,

$$\frac{\mathrm{d}i}{\mathrm{d}z} = (\beta S_0 - \alpha)i,\qquad(23)$$

and for the discrete part: $\forall k \in \mathbb{N}^*$,

$$i(k\tau^+) = S_0\left(1 - \exp\left(-\frac{\theta\pi\mathrm{e}^{-\mu(T-\tau)}}{\lambda}i(k\tau)\right)\right)$$

$$\cong S_0\frac{\theta\pi\mathrm{e}^{-\mu(T-\tau)}}{\lambda}i(k\tau),\qquad(24)$$

since i is assumed to be small. Proceeding as in van den Berg et al. (2011), Eqs. 23 and 24 also read:

$$\frac{\mathrm{d}i}{\mathrm{d}z} = \left(\beta S_0 - \alpha + \log\left(\frac{\theta\pi\mathrm{e}^{-\mu(T-\tau)}}{\lambda}S_0\right)\delta(t - k\tau)\right)i,$$
$$\qquad(25)$$

where δ is Dirac's delta function. Bacaer and Guernaoui (2006) showed that for a system such as Eq. 25, one obtains a basic reproduction number denoted R_0 such as:

$$\mathsf{R}_0 = \begin{cases} \dfrac{\beta S_0\tau}{\alpha\tau - \log\left(\dfrac{\theta\pi\mathrm{e}^{-\mu(T-\tau)}}{\lambda}S_0\right)} & \text{if } \dfrac{\theta\pi\mathrm{e}^{-\mu(T-\tau)}}{\lambda}S_0 < 1, \\[4ex] \dfrac{\beta S_0}{\alpha} & \text{if } \dfrac{\theta\pi\mathrm{e}^{-\mu(T-\tau)}}{\lambda}S_0 = 1, \\[4ex] \dfrac{\beta S_0\tau + \log\left(\dfrac{\theta\pi\mathrm{e}^{-\mu(T-\tau)}}{\lambda}S_0\right)}{\alpha\tau} & \text{if } \dfrac{\theta\pi\mathrm{e}^{-\mu(T-\tau)}}{\lambda}S_0 > 1. \end{cases}$$
$$\qquad(26)$$

Notice that $\mathscr{R}_0 > 1 \Leftrightarrow \mathsf{R}_0 > 1$. The difference is a matter of definition. In the body of the paper, we showed that $\mathscr{R}_0$ is the basic reproduction number of a primary inoculum unit. In other words, $\mathscr{R}_0$ is an ecological definition. R_0 is rather an epidemiological definition: It is the expected number of infections directly generated by a single infected individual introduced at a random time, in a disease-free context.

Interestingly, "Linearized model" section and van den Berg et al. (2011) strongly suggest that in the limit of infinitely small values of $\theta\pi\mathrm{e}^{-\mu(T-\tau)}/\lambda$, the strain that has the greatest epidemiological R_0 (rather than the largest ecological $\mathscr{R}_0$) is expected to eventually win the competition. See, e.g., (Mylius and Diekmann 1995) for related issues in a broader ecological context.

References

Abang MM, Baum M, Ceccarelli S, Grando S, Linde CC, Yahyaoui A, Zhan J, McDonald BA (2006) Differential selection on *Rhynchosporium secalis* during parasitic and saprophytic phases in the barley scald disease cycle. Phytopathology 96:1214–1222

Agrios G (2005) Plant pathology. Elsevier Academic, San Diego

Amarasekare, P (2003) Competitive coexistence in spatially structured environments: a synthesis. Ecol Lett 6:1109–1122

Auger P, Bravo de la Parra R, Poggiale JC, Sánchez E (2008) Aggregation methods in dynamical systems and applications in population and community dynamics. Phys Life Rev 5:79–105

Bacaer N, Guernaoui S (2006) The epidemic threshold of vector-borne diseases with seasonality. J Math Biol 53(3):421–436

Bailey DJ, Gilligan CA (1999). Dynamics of primary and secondary infection in take-all epidemics. Phytopathology 89:84–91

Carson ML (1998) Aggressiveness and perennation of isolates of *Cochliobolus heterostrophus* from North Carolina. Plant Dis 82:1043–1047

Chesson, P (2000) Mechanisms of maintenance of species diversity. Annu Rev Ecol Syst 31:343–366

Daval S, Lebreton L, Gazengel K, Guillerm-Erckelboudt AY, Sarniguet A (2010) Genetic evidence for differentiation of *Gaeumannomyces graminis* var. *tritici* into two major groups. Plant Pathol 59:165–178

Diekmann O, Hesterbeek JAP (2000) Mathematical epidemiology of infectious diseases: model building, analysis and interpretation. Wiley, Chichester

Fenwick DW (1949) Investigations on the emergence of larvae from cysts of the potato-root eelworm *Heterodera rostochiensis*. I. Technique and variability. J Helminthol 23:157–170

Fitt BDL, Huang YJ, van den Bosch F, West JS (2006) Coexistence of related pathogen species on arable crops in space and time. Annu Rev Phytopathol 44:163–182

Fournier E, Giraud T (2008) Sympatric genetic differentiation of populations of a generalist pathogenic fungus, *Botrytis cinerea*, on two different host plants, grapevine and bramble. J Evol Biol 21:122–132

Gadoury DM, Pearson RC (1990) Ascocarp dehiscence and ascospore discharge in *Uncinula necator*. Phytopathology 80:393–401

Gause, GF (1934) The struggle for existence. Williams and Wilkins, Baltimore

Gee LM, Stummer BE, Gadoury DM, Biggins LT, Scott ES (2000) Maturation of cleistothecia of *Uncinula necator* (powdery mildew) and release of ascospores in southern Australia. Aust J Grape Wine Res 6:13–20

Geritz SAH, Kisdi E (2004) On the mechanistic underpinning of discrete time population models with complex dynamics. J Theor Biol 228:261–269

Gubbins S, Gilligan CA (1997) Persistence of host-parasite interactions in a disturbed environment. J Theor Biol 188(2):241–258

Guckenheimer J, Holmes P (2002) Nonlinear oscillations, dynamical systems, and bifurcations of vector fields, applied mathematical sciences, vol 42. Springer, New York

Harrison JG (1992) Effects of the aerial environment on late blight of potato foliage—a review. Plant Pathol 41:384–416

Kiss L, Pintye A, Kovács GM, Jankovics T, Fontaine MC, Harvey N, Xu X, Nicot PC, Bardin M, Shykoff JA, Giraud T (2011) Temporal isolation explains host-related

genetic differentiation in a group of widespread mycoparasitic fungi. Mol Ecol 20:1492–1507. doi:10.1111/j.1365-294X.2011.05007.x

Lebreton L, Gosme M, Lucas P, Guillerm-Erckelboudt AY, Sarniguet A (2007) Linear relationship between *Gaeumannomyces graminis* var. *tritici* (Ggt) genotypic frequencies and disease severity on wheat roots in the field. Environ Microbiol 9:492–499

Madden LV, van den Bosch F (2002) A population-dynamics approach to assess the threat of plant pathogens as biological weapons against annual crops. BioScience 52(1):65–74

Madden LV, van den Bosch F (2007) The study of plant diseases epidemics. APS, Saint Paul

Mailleret L, Lemesle V (2009) A note on semi-discrete modelling in the life sciences. Philos Trans R Soc A 367:4779–4799

Montarry J, Cartolaro P, Delmotte F, Jolivet J, Willocquet L (2008) Genetic structure and aggressiveness of *Erysiphe necator* populations during grapevine powdery mildew epidemics. Appl Environ Microbiol 74:6327–6332

Montarry J, Cartolaro P, Richard-Cervera S, Delmotte F (2009) Spatio-temporal distribution of *Erysiphe necator* genetic groups and their relationship with disease level in vineyards. Eur J Plant Pathol 123:61–70

Mougou A, Dutech C, Desprez-Loustau ML (2008) New insights into the identity and origin of the causal agent of oak powdery mildew in Europe. For Pathol 38:275–287

Mougou Hamdane A, Giresse X, Dutech C, Desprez-Loustau ML (2010) Spatial distribution of lineages of oak powdery mildew fungi in France, using quick molecular detection methods. Ann For Sci. doi:10.1051/forest/2009105

Mylius SD, Diekmann O (1995) On evolutionarily stable life histories, optimization and the need to be specific about density dependence. Oikos 74:218–224

Rawsthorne D, Brodie B (1986) Root growth of susceptible and resistant potato cultivars and population dynamics of *Globodera rostochiensis* in the field. J Nematol 18:379–384

Shang H, Grau CR, Peters RD (2000) Oospore germination of *Aphanomyces euteiches* in root exudates and on the rhizoplanes of crop plants. Plant Dis 84:994–998

Shaw MW (1994) Seasonally induced chaotic dynamics and their implications in models of plant disease. Plant Pathol 43(5):790–801

Smith, RJ (2008) Modelling disease ecology with mathematics. American Institute of Mathematical Sciences, Springfield

Strömberg A, Boström U, Hallenberg, N (2001) Oospore germination and formation by late blight pathogen *Phytophthora infestans* in vitro and under field conditions. J Phytopathol 149:659–664

Truscott JE, Webb CR, Gilligan CA (1997) Asymptotic analysis of an epidemic model with primary and secondary infection. Bull Math Biol 59(6):1101–1123

Truscott JE, Gilligan CA, Webb CR (2000) Quantitative analysis and model simplification of an epidemic model with primary and secondary infection. Bull Math Biol 62(2):377–393

van den Bosch F, McRoberts N, van den Berg F, Madden LV (2008) The basic reproduction number of plant pathogens: matrix approaches to complex dynamics. Phytopathology 98(2):239–249

van den Berg F, Gilligan CA, Bailey DJ, van den Bosch F (2010) Periodicity in host availability does not account for evolutionary branching as observed in many plant pathogens: an application to *Gaeumannomyces graminis* var. *tritici*. Phytopathology 100:1169–1175

van den Berg F, Bacaer N, Metz JAJ, Lannou C, van den Bosch F (2011) Periodic host absence can select for both higher or lower parasite transmission rates. Evol Ecol 25(1):121–137

Webb CR, Gilligan CA, Asher MJC (1999) A model for the temporal buildup of *Polymyxa betae*. Phytopathology 89(1):30–38

Williams T, Beane J (1979) Temperature and root exudates on the cereal cyst-nematode *Heterodera avenae*. Nematologica 25:397–405

Wilson M and Lindow SE (1994) Coexistence among epiphytic bacterial populations mediated through nutritional resource partitioning. Appl Environ Microbiol 60:4468–4477